ACI STRUCTURAL JOURNAL TECHNICAL PAPER

Title No. 112-S42

Seismic Performance of Precast Recycled Concrete Frame Structure

by Jianzhuang Xiao, Tao Ding, and Thi Loan Pham

Shake-table tests on a six-story precast recycled aggregate concrete (RAC) space frame structure were investigated. The 1/4-scale precast RAC frame structure was constructed with precast beams, precast columns, and cast-in-place (CIP) slabs, which is different from the previous CIP RAC frames researched. Based on the structural dynamic responses, the failure pattern and mechanism, deformation, and energy dissipation capacity were analyzed and evaluated. Furthermore, the seismic damage assessment of the entire precast structure was completed. The evaluation on the interstory and residual drifts, displacement ductility, and energy dissipation indicate that the frame had comparable deformation ability to that of a natural aggregate concrete (NAC) precast frame and was able to dissipate the input energy during earthquakes. The RAC frame model did not collapse at the maximum considered earthquake level, suggesting that the precast RAC frame structure had enough collapse-resistant capacity during earthquake attacks, which is also proved by the seismic damage assessment.

Keywords: damage assessment; frame structure; precast; recycled aggregate concrete (RAC); seismic performance; shake-table tests.

INTRODUCTION

The recycling of waste concrete is seen as one of the best ways to combat the rapid increase in the generation of construction and demolition waste concrete. Waste concrete is crushed and processed into aggregates that are then used as a constituent of coarse aggregates in newly cast concrete. This is referred to as recycled aggregate concrete (RAC). This area of research has received much attention recently.[1,2] In fact, researchers from China and countries worldwide have engaged in many investigations on the physical and mechanical properties of RAC. Achievements summarized by Nixon,[3] Hansen,[4,5] ACI 555R-01,[6] Xiao et al.,[7] and Poon and Chan[8] revealed that some mechanical properties of RAC may be generally lower than those of natural aggregate concrete (NAC), and the recycled coarse aggregate (RCA) replacement percentage has a considerable influence on the stress-strain relationship of RAC under uniaxial compression and tensile loadings.[7] However, due to the advanced mixture design procedure or RCA replacement methodology, some researchers, such as Dhir et al.,[9] Fathifazl et al.,[10] and Topcu and Şengel[11] found that some mechanical properties of RAC are even superior or equal to the NAC.

To apply RAC as a structural material, a series of experimental studies on the structural behavior of RAC components and structures have also been carried out. Studies on RAC beams undertaken by Sato et al.[12] and Fournier et al.[13] concluded that the shear capacity of reinforced RAC beams is comparable, or even superior, to that of beams made entirely with NAC. Tests investigated by Choi et al.[14] proved that the axial behavior exhibited in RAC columns is comparable to that found in NAC columns, and the reinforced concrete columns constructed with RAC can be used as load-bearing structural elements. Corinaldesi and Moriconi[15] and Corinaldesi et al.[16] found that frame joints prepared with 100% and 30% RCAs replacing natural coarse aggregates (NCAs) both showed adequate structural behavior if the joints are properly designed. Recently, four 1/2-scale plane frames made of RAC under low-frequency cyclic lateral load and one CIP RAC space frame shake-table tests were studied by the authors.[17,18] According to the two investigations, although the overall seismic behavior of RAC structure declines with an increase of the RCAs' replacement percentage, RAC structures with corresponding mixture proportions and construction details are still able to resist an earthquake attack in general. The positive results of these pioneer studies further support and encourage the application of RAC in structures for engineering projects.

It is noticed that most current studies focused on monolithic (wholly CIP) RAC structures and the topics on seismic performance of precast RAC structures seem to have been ignored. In fact, precast concrete structures made of NAC have already been widely studied and promoted in many countries worldwide, especially in the United States, New Zealand, and Japan, where moderate-to-severe earthquakes often occur. In the 1990s, a 60%-scale, five-story precast NAC building that was tested under simulated seismic loading in the United States[19] confirmed that the behavior of this kind of structure was extremely satisfactory. Two full-scale precast NAC subframes and one monolithically cast NAC subframe subjected to quasi-static simulated seismic loading were investigated by Khoo et al.[20] Their findings showed that the precast NAC frames exhibited good ductility and provided fine moment-resisting behavior. Other investigations undertaken by Xue and Yang,[21] Alcocer et al.,[22] and Psycharis and Mouzakis[23] all proved that the precast NAC frame structures were capable of matching the overall performance with that of the monolithic frames.

There is a common view that prefabrication could offer improved quality control and higher opportunities for standardization of concrete structures. Prefabrication combined

ACI Structural Journal, V. 112, No. 4, July-August 2015.
MS No. S-2014-156.R1, doi: 10.14359/51687660, received September 18, 2014, and reviewed under Institute publication policies.

with modular design and standard precast elements can give good results, and the quality of RAC components may be ensured if the prefabrication technique is applied in RAC structures. Secondly, according to the investigation done by Jaillon and Poon[24] and Tam et al.,[25] prefabrication can provide a better solution to the problem of large waste concrete for on-site activities. Adoption of prefabrication has potential in the construction industry and the long-term construction costs can be reduced. Therefore, structural systems employing precast concrete elements made of RAC might promote the popularization of RAC and conform to the trend of industrialization or sustainable development.

In fact, applying RAC into precast products had also caught the attention of engineers and contractors, and some positive achievements have been made by Soutsos et al.[26,27] Semi-precast columns[28] and semi-precast beams[29] with RAC showed that semi-precast elements with RAC have similar structural behavior to that of NAC elements. However, to the best knowledge of the authors, there are still no systematic evaluations focusing on the overall seismic performance of precast RAC structures, and this is the initial purpose and motivation of this investigation.

RESEARCH SIGNIFICANCE

This paper presents the first shake-table test on a precast RAC frame to evaluate the overall seismic performance and accumulate experimental evidence for establishing related design guidelines for such frame structures. This investigation attempts to give some insights into the entire seismic performance of the precast RAC frame according to analysis on its failure pattern, stiffness degradation, energy dissipation, and seismic damage assessment. The analysis results will promote the safety of prefabricated structures and may also further support the popularization of RAC structures in civil engineering.

DETAILS OF SHAKE-TABLE TESTS

Design and construction details

To get an intensive understanding of the seismic performance of the RAC frame structure if prefabricated, one 1/4-scaled, two-bay, two-span, and six-story RAC frame structure was constructed, where the general geometry, the element sections, and corresponding reinforcement of the model were all the same with the previous CIP model investigated by the authors. The reinforcement and element details of the tested model were also the same with the previous CIP model, satisfying the seismic detailing requirements of ACI 318-05.[30] The details are shown in Fig. 1(a) to (c) (more information can also be found in Reference 18). The similarity relations between the prototype and the model were derived from Buckingham π theorem[31] and the main parameters are listed in Table 1.

It is worth mentioning that the construction process for the precast RAC frame structure included two steps: fabricating precast components and constructing the entire model. Beams were designed as semi-precast beams[29] and the top reinforcements of beams were assembled at the construction site. The construction process was started after 54 precast columns and 72 beams were cast and cured at the ambient temperature for 28 days. Welding connection was adopted for longitudinal reinforcing bars of precast columns in the joint area. The reinforcements of the inner joints and one typical configuration of the assembled joint can be seen in Fig. 1(d) and (e). After the precast beams were erected at the head of precast columns and the slab reinforcements were fixed in the forms, ready mixed RAC was then poured in place for the joints and slabs. The entire constructed precast RAC model is shown in Fig. 1(b).

Materials

Materials selection was also the same with the previous CIP model investigation.[18] The fine aggregates used were river sand with particle diameter of 0.002 to 0.197 in. (0.05 to 5 mm). The coarse aggregates used were RCAs with particle diameters of 0.197 to 0.394 in. (5 to 10 mm). RCAs were produced from demolished building concrete and most of the compressive strength for demolished concrete was approximately 3.626 ksi (25 MPa). For the first step, large pieces of concrete were crushed and residual reinforcement was removed by hydraulic machine. Before the RCAs were mixed in the new concrete, it was cleaned by tap water as the second step in order to remove the clay on the surface, which is a much different process than that when using natural aggregates. The recycled concrete mixture, with a nominal strength grade of C30 and a slump flow value in the range of 7.087 to 7.874 in. (180 to 200 mm), was proportioned with the RCA replacement percentage equal to 100% (that is, all the coarse aggregates were RCAs). The RAC mixture proportion was water:cement:sand:RCAs = 1:1.859:3.202:4.554. The compressive strength and elastic modulus of RAC was tested before the earthquake test in order to give a better understanding of the material behavior of this model. Table 2 presents the mechanical properties of RAC, showing that the elastic modulus of RAC is 20% lower than that of NAC. Galvanized steel wires of No. 8 (diameter of 0.1552 in. [3.94 mm]) and No. 10 (diameter of 0.1308 in. [3.32 mm]) were adopted as the longitudinal reinforcement and No. 14 (diameter of 0.091 in. [2.32 mm]) for transversal reinforcement in the precast model according to the similitude laws of the frame model. The yield strengths of No. 8, No. 10, and No. 14 were 51.9235, 44.3815, and 36.5495 ksi (358, 306, and 252 MPa), respectively.

Test procedure

Consistent with the previous studies focusing on CIP research,[18] Wen Chuan wave (WCW, 2008, N-S), El Centro wave (ELW, 1940, N-S), and Shanghai artificial wave (SHW) were selected as the input seismic waves. WCW and ELW could be considered for very dense soil and soft rock area, while SHW is for the soft soil areas. The time-history of inputs including WCW, ELW and SHW can be found in Reference 18. In addition, the order was WCW → ELW→ SHW during the test process. The tests were performed with the main excitation in the x-direction, shown in Fig. 1(a), to evaluate overall seismic performance of the RAC frame structure.

The test program of the shake-table tests consisted of seven phases—that is, tests for peak ground acceleration (PGA)

Table 1—Similitude scale parameters

Parameter	Length	Acceleration	Elastic modulus	Time	Damp	Density
Model/prototype	0.250	1.848	1.000	0.368	0.092	2.164

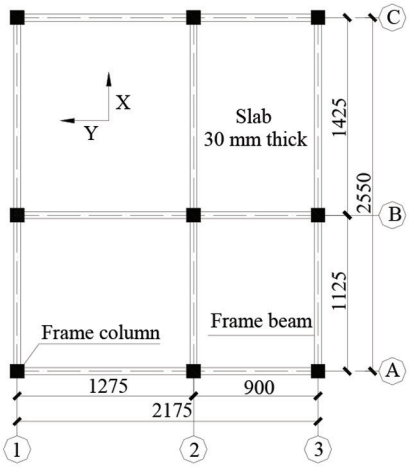

(a) Plan layout

(b) Precast model on the shaking table

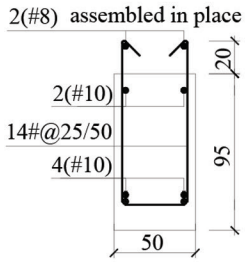

Beam section

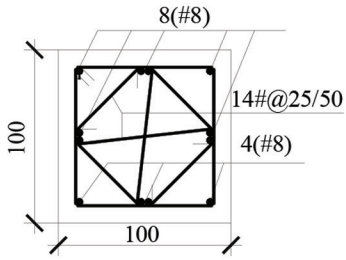

Corner column section

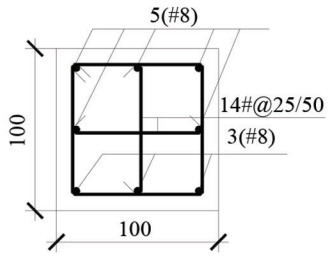

Side and center column section

(c) Reinforcements for the frame beams and columns

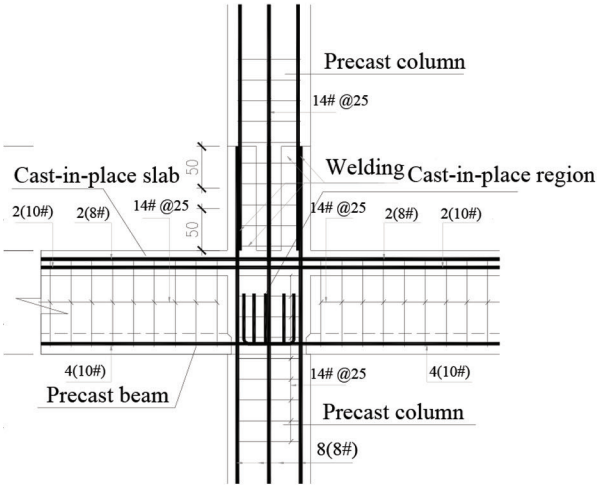

(d) Reinforcements for inner joint

(e) Typical configuration of the assembled joint

Fig. 1—Configuration and reinforcement for precast RAC frame model. (Note: Units in mm; 1 mm = 0.0394 in.)

of 0.066*g*, 0.130*g*, 0.185*g*, 0.370*g*, 0.415*g*, 0.550*g*, and 0.750*g*. According to Appendixes G and I of the Seismology Committee[32] and the revisions proposed for Appendix in the SEAOC Performance-Based Seismic Engineering Ad Hoc Subcommittee,[33] the seismic action were identified as four earthquake intensity levels EQ-1 (0.066 *g*-intensity 7; 0.130 *g*-intensity 8), EQ-2 (0.185 *g*-intensity 7; 0.370 *g*-intensity 8), EQ-3 (0.415 *g*-intensity 7; 0.550 *g*-intensity 8),

Table 2—Mechanical properties of recycled aggregate concrete

Apparent density of RCA, lb/yd^3 (kg/m^3)	Water absorption of RCA, %	Compressive strength of RAC, ksi (MPa)	Elastic modulus of RAC, ksi (GPa)
4180.3 (2480)	8.21	5.366 (37.0)	3422 (23.6)

and EQ-4 (0.750 *g*-intensity 8). These four levels of earthquakes are characterized as frequent, occasional, rare, and maximum considered events, having a mean return period of 25, 72, 250 to 800, and 800 to 2500 years, respectively.

For the purpose of monitoring the local behaviors of RAC strains, 24 strain gauges were installed on the bottom of the columns from the first to the third story. A total of 30 accelerometers, including two on the base beams, four on each story from the first to fifth story, and eight on the roof were set to record the horizontal accelerations. A total of 14 displacement linear variable differential transformers (LVDTs) were installed including two on each story from the first to fifth story and four on the roof, and all the displacement gauges were arranged to record the horizontal displacements. Figure 2 displays the arrangement of these sensors throughout the tests.

Failure pattern and mechanism

For the local behaviors of the frame model, the measured maximum strain was 1264 με with a PGA of 0.130*g*, when the first crack was observed on the beams, according to the strain gauge readings for concrete. During the test phase with a PGA of 0.415*g*, the measured maximum compressive strain of RAC was 1926 με, which was very close to the peak compressive strain of RAC.[7,34] The development of RAC compressive strain agreed well with the failure progress of the frame.

The main vertical cracks first appeared on beam ends of the frame from the first to third story consistent with the strain gauge readings that the maximum strain was 1264 με, shown in Fig. 3(a). Cracks occurring at column ends at the later stage of the tests were primarily horizontal cracks at first and second stories, which can be seen in Fig. 3(b). For the joints, more fine horizontal and shear cracks spread on part of the CIP joints in the first and second stories (Fig. 3(c)), leading to a serious damaged condition of the precast frame at the end of the earthquake tests. This phenomenon illustrates that more effective measures such as increasing the reinforcement or RAC strength grade should be taken to improve the integrity of the structure in an actual engineering project.

During the entire shake-table tests, it was observed that the first plastic hinge occurred at the first-story beam end, then at the second-story beam end, as expected. In general, the precast RAC frame exhibited a mixed sidesway mechanism similar to the NAC frame tested by Park and Paulay[35] and failed due to concrete crushing and buckling of longitudinal bars, which is very similar to previous investigations focusing on a 60%-scale five-story precast NAC building completed by Priestley et al.[19] and a half-scale, two-story precast NAC frame structure investigated by Xue and Yang.[21] Figure 3(d) also presents a typical failure pattern of precast NAC joint.[22] It can be clearly seen from Fig. 3(d)

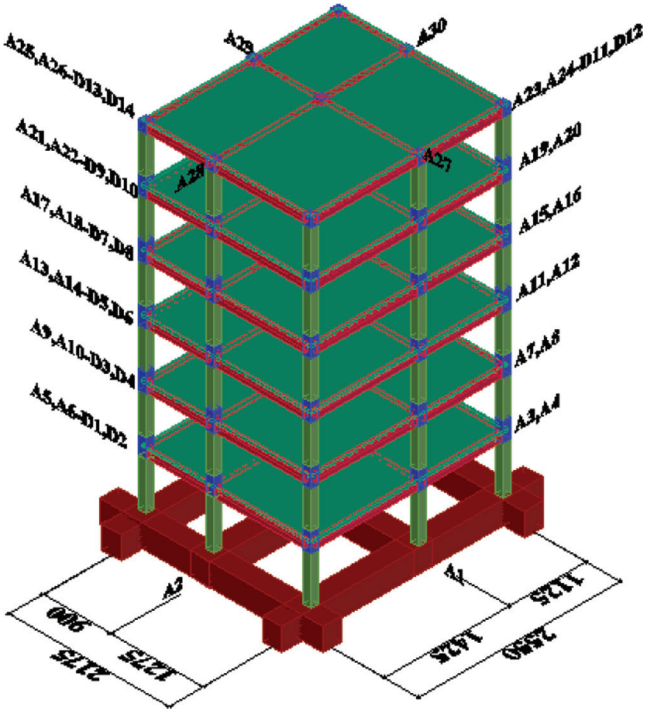

Fig. 2—Arrangement of accelerometers and displacement gauges. (Note: Units in mm; 1 mm = 0.0394 in.)

that the crack pattern of joints in precast frame made of RAC is relatively similar to that of precast frame made of NAC.

SEISMIC PERFORMANCE EVALUATION

Interstory drift and residual drift

Based on the guidance given in the SEAOC Blue Book,[32] the following drift limits were used as acceptable values to evaluate the frame performance at the aforementioned four earthquake intensity levels: the maximum transient interstory drifts of 0.5% (EQ-1), 1.5% (EQ-2), 2.5% (EQ-3), and 3.8% (EQ-4); and the maximum residual drifts of 0.1% (EQ-1), 0.3% (EQ-2), 0.5% (EQ-3), and 0.75% (EQ-4), respectively.

The maximum transient interstory drifts obtained from the LVDTs on each story during the shake-table tests are summarized in Fig. 4. It is shown that the precast frame structure exhibited acceptable performance in terms of the maximum transient interstory drift at an earthquake intensity of 7, which was typically governed by the first- or second-story lateral interstory displacement. A similar phenomenon could also be observed in the research done by Priestley et al.[19] as well as Rahman and Sritharan,[36] who focused on precast NAC structures.

For the EQ-1 and EQ-2 levels, the frame exhibited maximum interstory drifts lower than the acceptable value both at earthquake intensities of 7 and 8. For the following level of EQ-3, the maximum transient drifts at an earthquake intensity of 8 were a little higher and closer to the limitation of 2.5%, which was the target design drift. It should be noted that the precast RAC frame structure exhibited transient interstory drifts of up to 5.9%, which was much greater than the acceptable value of 3.8% at the level of EQ-4. In response to observing such a high interstory drift, it is worth noting that the precast NAC frame structure tested

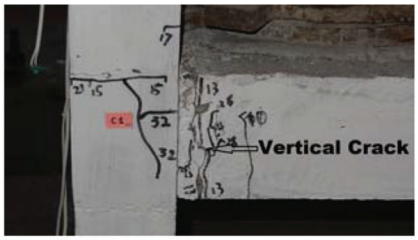

(a) Cracks on the RAC beam end

(b) Cracks on the RAC column base

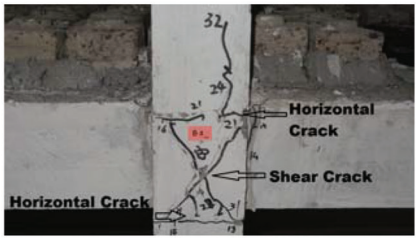

(c) Cracks on the RAC inner joint

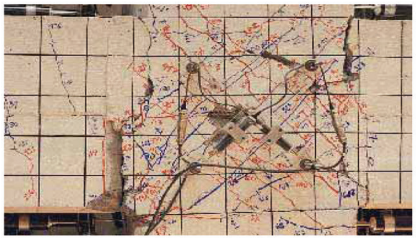

(d) Cracks on the NAC inner joint [22]

Fig. 3—Typical cracks on precast RAC and NAC frame structure.

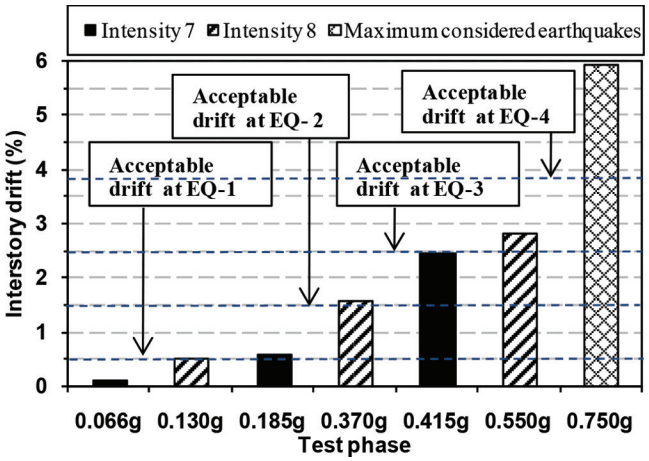

Fig. 4—Maximum interstory drift.

by Priestley et al.[19] was subjected to a maximum interstory drift of 4.5%.

In addition, the residual drifts of the precast RAC frame subjected to maximum considered earthquake motions were only 0.05%, which were found to be negligible and far below the acceptable limits. The recentering behavior of the precast frame systems was believed to be responsible for minimizing the residual drifts. The same results were also found in the tests by Priestley et al.[19]: that the residual drifts after the design level excitation were also very low—only 0.06%, as anticipated. The low residual drift is a significant advantage for both precast RAC and NAC frame structures over conventional CIP reinforced concrete construction, where very high residual drifts are possible.[19,37]

Hysteretic curves

Figure 5(a) depicted the expected lateral base shear force versus roof drift (lateral displacement at roof divided by total frame height) hysteretic response of the overall frame. Moreover, as the first and second stories are the sensitive stories of the frame model, the interstory shear force versus interstory drift hysteretic response for the first and second stories, in particular, are also plotted in Fig. 5(b) and (c), respectively.

It can be found that the areas of hysteretic curves became gradually larger due to the increasing drift, showing an acceptable energy dissipation capacity, with roof and interstory drift increasing and plastic hinges mainly forming at beam ends in the first and second stories. At the earlier stage, before the cracking point, envelopes of the hysteretic curves were basically linear, indicating that the structure remained in the elastic state. After cracks appeared in the model, slight pinching was noticed in the hysteretic curves with a PGA of 0.185 *g* after the roof drift level of 0.35%; this was primarily due to column-end and beam-end cracking as well as concrete softening and the bond-slip influence. The pinch effect on the hysteric curves can be observed somewhat obviously in the later test phases because the model went into the nonlinear stage and underwent the shear deformation. Similar results were often obtained in precast NAC frame structures.[21,23,38]

Capacity curves and displacement ductility

Generally, the capacity curve can reflect the variation of the lateral capacity of the structure. The capacity curve of the tested precast RAC frame model structure was obtained through fitting with the form of an exponential function, as shown in Fig. 6. According to the capacity curve, in the test phase with a PGA of 0.415*g*, the base shear of the model was close to its maximum value according to the capacity curve. Furthermore, from the capacity curve, the yield loading point, maximum loading point, and ultimate loading point can be easily recognized. A ductility coefficient was defined in this study to evaluate the deformation ability of the overall precast RAC frame structure. It is expressed as follows

$$\mu = \theta_u/\theta_y \quad (1)$$

where the yield drift θ_y can be determined according to the criteria suggested by Park[39]; and the ultimate drift θ_u can be

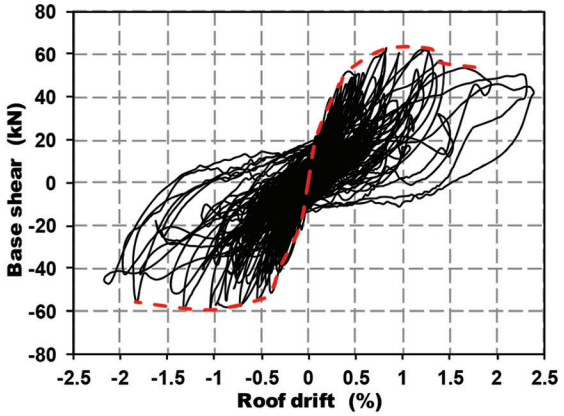

(a) Hysteretic curves of the roof of the whole test

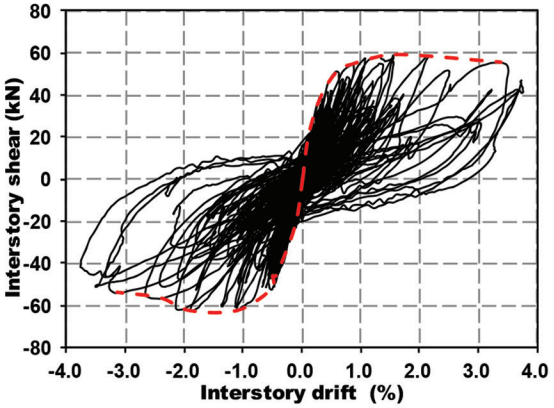

(b) Hysteretic curves of the 1st story of the whole test

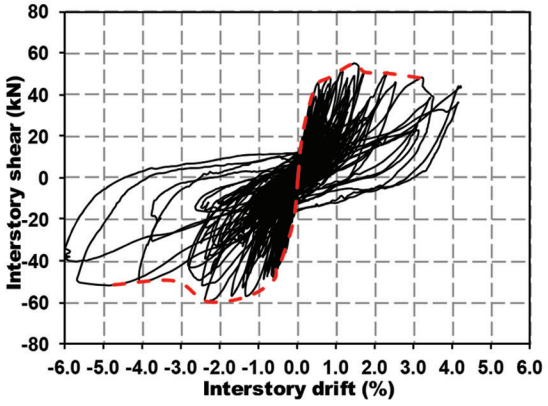

(c) Hysteretic curves of the 2nd story during the whole test

Fig. 5—Hysteretic curves of precast RAC frame structure. (Note: 1 kN = 0.2248 kip.)

determined by the test, at which point the base shear is close to 85% of the maximum value.

Therefore, the ductility coefficient was determined as 3.852 according to Eq. (1). The result reveals that the precast RAC frame model has an adequate ductility to withstand a maximum considered earthquake level. Many related experimental investigations and theoretical analysis show that the displacement ductility coefficient of the concrete structures is generally between 3 to 5.[35] It is revealed by this evaluation that the precast RAC frame structure has very similar

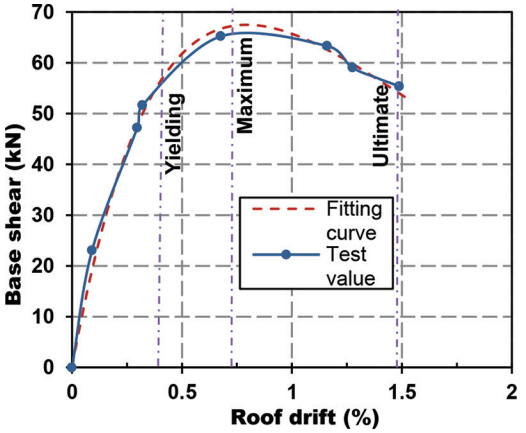

Fig. 6—Capacity curves of precast RAC frame structure. (Note: 1 kN = 0.2248 kip.)

displacement ductility and deformation ability as precast NAC frames.[18]

Stiffness degradation

To assess the stiffness degradation of the model, the secant stiffness was adopted, which was calculated by a straight line between the maximum load and corresponding displacement points for the pull and push directions. The rules for stiffness degradation are shown in Fig. 7 and explained in the following:

1. The overall frame and the first- or second-story stiffness degradation tendency were similar to each other in general.

2. The story stiffness decreased dramatically at the early stage of the shake-table tests compared to the entire frame stiffness. For an example, in the phase with the PGA of 0.130 *g*, the stiffness ratio for the first or second stories was only about 60% compared to the initial stiffness; however, the entire frame stiffness decreased to 90% of the initial overall stiffness. This proves that the frame stiffness decreased relatively more slowly, which could be contributed to the fact that most of the cracks occurred at the first and second stories.

3. At the end of the test, the stiffness dropped approximately by 84%, 92%, and 93% for the overall, first story, and second story, respectively, showing that the frame structure experienced remarkable damage. The frame structure significantly performed large deformation due to the considerable stiffness degradation of the first and second stories.

4. As a whole, the stiffness continuously decreased with an increase of PGA throughout the test, and stiffness degradation was relatively faster during the middle stage of the tests.

Energy dissipation capacity

The amount of cumulative energy dissipated for the precast RAC frame structure is plotted versus the roof drift according to integral calculation on hysteretic curves for each story in Fig. 8. It is observed from the figure that:

1. The energy dissipation of the first story was almost equal to that of the second story, and the sum of the energy dissipation of both the first and second stories accounted for approximately 60% of the total energy consumption in general.

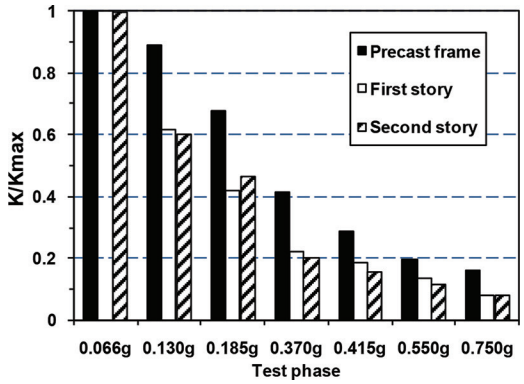

Fig. 7—Stiffness degradation of precast RAC frame structure.

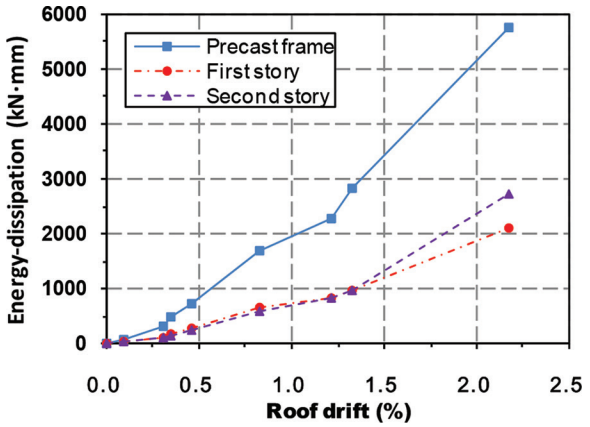

Fig. 8—Energy-dissipation curve of precast RAC frame structure. (Note: 1 kN·mm = 8.85 × 10^{-3} kip·in.)

2. The amount of energy dissipated was very small during the early stage of the tests. The amount of energy dissipated at the roof drift of 0.3% was only approximately 5% of that at the roof drift of 2.2% for the global model.

3. During the later stage of the test when the frame entered into the elasto-plastic stage, the energy dissipation capacity of the tested frame dramatically increased, though the load increased slowly and even decreased with the increasing PGA. The good energy dissipation capacity proved the favorable capacity of the structure to perform satisfactorily during the elasto-plastic stage.

4. In general, the energy dissipation capacity of the precast RAC frame structure was enough to absorb and dissipate the input energy during the earthquake action so as to guarantee the safety of the structure.

Seismic damage assessment

In this study, the different damage states of a concrete frame structure were identified based on the Park and Ang global damage indexes[40] of the overall structure. The ranges of the Park and Ang's index for different damage states have been established to reflect damage to concrete frames more realistically and are presented in Table 3. According to Park et al.,[41] the seismic structural damage may be expressed as a linear combination of the maximum deformation and the hysteretic energy expressed in terms of the damage index

Table 3—Ranges of Park and Ang's[40] damage index for different damage states

Damage state	None	Minor	Moderate	Severe	Collapse
Range of index	0.0 to 0.1	0.1 to 0.2	0.2 to 0.5	0.5 to 1.0	>1.0

$$D = \frac{\delta_M}{\delta_u} + \frac{\beta}{Q_y \delta_u} \int dE \tag{2}$$

where D is the damage index, an empirical measure of damage ($D > 1.0$ indicates total damage or collapse); δ_M is the maximum response deformation; δ_u is the ultimate deformation ability under static loading; Q_y is the calculated yield strength; dE is the incremental absorbed hysteretic energy; and β is the coefficient for cyclic loading effect (function of structural parameters).

Damage index D for each story was obtained from the damage index D for each structural element, weighted by the energy-absorbing contribution factor λ_i, and is expressed as

$$D = \sum_{i}^{n} \lambda_i D_i \tag{3}$$

where $\lambda_i = E_i / \sum E_i$; and E_i is the total absorbed energy at the story i, $n = 6$ in this investigation.

Similarly, the same method can be adopted to calculate the overall damage index D for the investigated precast RAC frame structure based on the damage index D for each story. Figure 9 presents the global structural damage index versus the corresponding PGA in different test phases. Combined with Table 3, it can be inferred from the figure that, for the level of EQ-1 as a frequently occurring earthquake, the overall damage index is 0.03 and 0.09 with the PGAs of 0.066*g* (intensity 7) and 0.130*g* (intensity 8), respectively—less than the limit value of 0.1, indicating that the frame maintained in the elastic stage and in an intact condition. For the next level of EQ-2 as an occasionally occurring earthquake, the overall damage index is just 0.11 with the PGA of 0.185*g* (intensity 7)—less than the limit value of 0.2, suggesting that the frame suffered minor damage; however, the overall damage index is 0.29 with the PGA of 0.370*g* (intensity 8), illustrating that the frame had been moderately damaged. For the level of EQ-3 as a rarely occurring earthquake, the overall damage index is 0.43 with the PGA of 0.415*g* (intensity 7), suggesting that the frame was still in a moderately damaged state; however, the overall damage index is 0.52 with the PGA of 0.550*g* (intensity 8), indicating that the frame had been severely damaged. When the model was subjected to the maximum considered events with a PGA of 0.750*g*, the damage index was 0.78, which is less than the collapse value of 1.0, and this is consistent with the test phenomenon.

It can be concluded from the damage assessment that the precast RAC frame structure was damaged more severely under the earthquake intensity of 8 than that under intensity of 7. However, the model did not collapse even in the

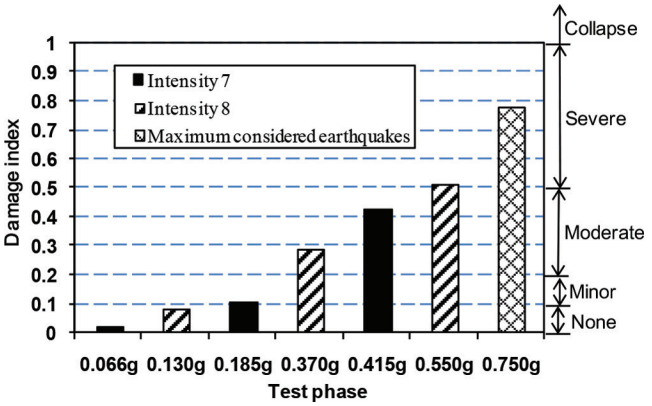

Fig. 9—Structural damage index under different test phase.

maximum considered earthquake, proving that the precast RAC frame structure possessed comparable deformation ability and seismic performance to the precast NAC frame structure.[36]

DISCUSSIONS

Compared with the previous research on a CIP RAC frame structures by the authors,[18] the geometry, material properties, and reinforcement of the tested model in this investigation were almost the same. Discussion about the comparison of the seismic behavior of the two models is presented in the following:

1. In the late nonlinear stage, after the frames suffered several strong earthquake attacks, the damage level of the post-cast joint is relatively more serious than that of CIP frame with more cracks and plastic hinges at the end of beams. The failure pattern of precast frame could be seen in Fig. 3 and more photos on the failure pattern of CIP frame can be found in Reference 18.

2. Comparisons of the maximum interstory drift between precast and CIP RAC frame are displayed in Fig. 10. It is proved that the maximum interstory drift of the precast RAC structure is larger than that of the wholly CIP RAC structure at each test phase except 0.550*g*. Specially, at the 0.750*g* stage, the maximum interstory drift is 71% larger than the drift level of the CIP RAC frame.[18] However, there was no indication that the frame would collapse at this drift level.

3. The hysteretic curves of the two models indicate that both the CIP and precast RAC frames have good capability of energy consumption. Figure 11 presents the comparisons of stiffness degradation. It can be seen from Fig. 11 that the stiffness of precast frame decreases faster than that of the CIP frame during the final test phases. Calculation on the ductility proves that both of the two structures show favorable seismic performance.[18]

4. The CIP and precast RAC frame structures did not collapse during the shake-table tests. For the post-cast joint of precast RAC frame, to improve the shear capacity and prevent cracks or damages occurring between the construction interface, roughening treatments and shear connectors could be set on the composition plane, or advanced connection technology such as grout sleeve connection could be applied, so as to strengthen the shear transfer between the post-cast joint and precast concrete elements in the joint

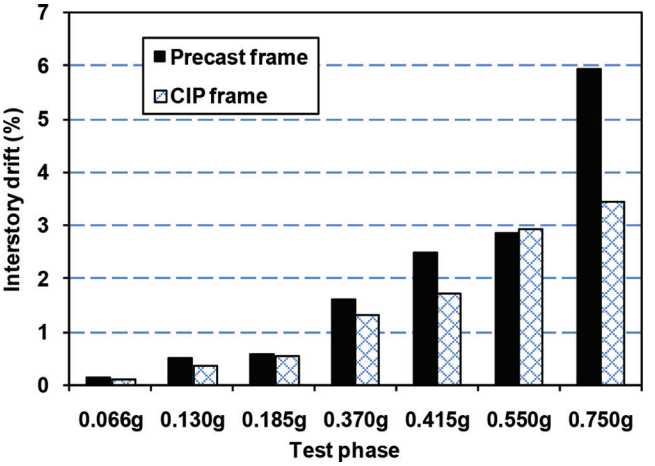

Fig. 10—Comparisons of maximum interstory drift.

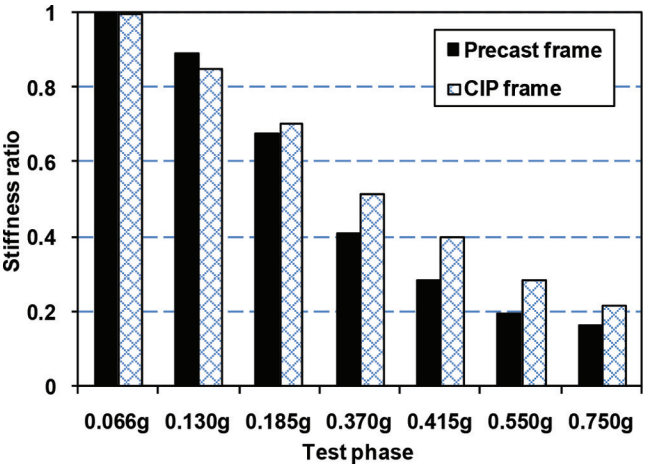

Fig. 11—Comparisons of stiffness degradation.

area. It is believed that these measurements will enhance the overall seismic behavior for precast frames. How to strengthen the energy consumption capacity of post-cast joints in the precast frame is the main area of future research.

5. Due to the decreasing durability of RAC,[42] the relative inferior durability aspects of the RAC structure should also be considered if it is applied in real projects. In fact, precast RAC elements that are prefabricated present a solution to enhance the durability of RAC structures. As stated previously, semi-precast columns[28] and semi-precast beams[29] with RAC showed similar structural behavior to that of NAC elements. However, the inferior durability of RAC could be avoided, as the RAC is located at the inner part of the components and not directly exposed to the environment. To the post-cast joint of RAC, optimizing the mixture proportion and adopting the double mixing method could improve the durability of RAC.

CONCLUSIONS

The comprehensive evaluation on the seismic performance of one precast RAC frame model structure was presented in this paper, including the failure pattern, deformation ability, stiffness degradation, energy dissipation capacity, and seismic damage assessment. Based on the positive results compared to those of NAC precast frame structure and a

wholly CIP RAC frame structure, the following conclusions are drawn:

1. The precast RAC frame structure, as expected, produced a mixed sidesway mechanism that was similar to the previous research on precast NAC frame structures. For the local behaviors, horizontal and shear cracks spread on part of the CIP joints in the first and second stories, illustrating that more effective measures such as increasing the reinforcement or RAC strength grade should be taken to improve the integrity of the structure in an actual engineering project.

2. The analysis on interstory and residual drift proves that the frame exhibited acceptable maximum transient interstory drift and the residual drifts were found to be negligible, revealing that the precast RAC frame structure has comparable collapse-resistant capacity to that precast NAC structure. It is also proved that the maximum interstory drift of the precast RAC structure is larger than that of the CIP RAC structure. In addition, the maximum lateral interstory drifts were typically governed by the first or second story, which proved that the first and second stories were both sensitive stories of the precast RAC frame structure.

3. Based on the analysis of hysteretic and capacity curves, the calculated global displacement ductility of the precast RAC frame was 3.852. The results show that overall seismic behavior of the precast RAC structure has no significant discrepancy compared to precast NAC structures. In addition, the stiffness of the frame continuously decreased with an increase of PGA due to the cumulative damage in columns and beams throughout the test due to the considerable stiffness degradation of the first and second stories.

4. In general, the sum of the energy dissipation for the first and second stories accounted for approximately 60% of total energy consumption. Moreover, the amount of energy dissipated was very small during the early stage of the tests; however, the energy dissipation capacity of the tested frame increased obviously during the later stage of the test. As a whole, the energy dissipation capacity of the precast RAC frame structure was favorable and the frame was able to absorb and dissipate the input energy during earthquake attacks so as to guarantee the safety of the structure.

5. The damage assessment of the precast RAC frame structure illustrates the structure was damaged more severely under the earthquake intensity of 8 than that under the intensity of 7. The maximum damage index is 0.78—less than 1.0—when the model was subjected to the maximum considered earthquake action, which is consistent with the test observations that the model did not collapse.

AUTHOR BIOS

Jianzhuang Xiao *is a Professor in the Structural Engineering Department at Tongji University, Shanghai, PR China, where he received his PhD in structural engineering. His research interests include the material properties and structural behavior of recycled concrete.*

Tao Ding *is a PhD Candidate in the Structural Engineering Department at Tongji University. His research interests include seismic performance of precast recycled concrete structures.*

Thi Loan Pham *has a PhD in the Structural Engineering Department at Tongji University. Her research interests include seismic response of recycled concrete structures.*

ACKNOWLEDGMENTS

The authors wish to acknowledge the financial support from the National Natural Science Foundation of China (NSFC) (No: 51325802, 51438007).

REFERENCES

1. Eguchi, K.; Teranishi, K.; Nakagome, A.; Kishimoto, H.; Shinozaki, K.; and Narikawa, M., "Application of Recycled Coarse Aggregate by Mixture to Concrete Construction," *Construction and Building Materials*, V. 21, No. 7, 2007, pp. 1542-1551. doi: 10.1016/j.conbuildmat.2005.12.023

2. Xiao, J., *Recycled Concrete*, Chinese Building Press, Beijing, China, 2008, 194 pp. (in Chinese)

3. Nixon, P. J., "Recycled Concrete as an Aggregate for Concrete—A Review," *Materials and Structures*, V. 11, No. 65, 1978, pp. 371-378.

4. Hansen, T. C., "Recycled Aggregate and Recycled Aggregate Concrete, Second State-of-the-Art Report: Developments from 1945-1985," *Materials and Structures*, V. 19, No. 3, 1986, pp. 201-246. doi: 10.1007/BF02472036

5. Hansen, T. C., *Recycling of Demolished Concrete and Masonry*, E&FN Spon, London, UK, 1990, 336 pp.

6. ACI Committee 555, "Removal and Reuse of Hardened Concrete (ACI 555R-01)," American Concrete Institute, Farmington Hills, MI, 2001, 26 pp.

7. Xiao, J. Z.; Li, J. B.; and Zhang, C., "Mechanical Properties of Recycled Aggregate Concrete under Uniaxial Loading," *Cement and Concrete Research*, V. 35, No. 6, 2005, pp. 1187-1194. doi: 10.1016/j.cemconres.2004.09.020

8. Poon, C. S., and Chan, D., "The Use of Recycled Aggregate in Concrete in Hong Kong," *Resources, Conservation and Recycling*, V. 50, No. 3, 2007, pp. 293-305. doi: 10.1016/j.resconrec.2006.06.005

9. Dhir, R. K.; Limbachiya, M. C.; and Leelawat, T., "Suitability of Recycled Concrete Aggregate for Use in BS 5328 Designated Mixes," *Proceedings of the ICE—Structures and Buildings*, V. 134, No. 3, 1999, pp. 257-274.

10. Fathifazl, G.; Abbas, A.; Razaqpur, A. G.; Isgor, O. B.; Fournier, B.; and Foo, S., "New Mixture Proportioning Method for Concrete Made with Coarse Recycled Concrete Aggregate," *Journal of Materials in Civil Engineering*, ASCE, V. 21, No. 10, 2009, pp. 601-611. doi: 10.1061/(ASCE)0899-1561(2009)21:10(601)

11. Topcu, I. B., and Şengel, S., "Properties of Concretes Produced with Waste Concrete Aggregate," *Cement and Concrete Research*, V. 34, No. 8, 2004, pp. 1307-1312. doi: 10.1016/j.cemconres.2003.12.019

12. Sato, R.; Maruyama, I.; Sogabe, T.; and Sogo, M., "Flexural Behavior of Reinforced Recycled Concrete Beams," *Journal of Advanced Concrete Technology*, V. 5, No. 1, 2007, pp. 43-61. doi: 10.3151/jact.5.43

13. Fournier, B.; Razaqpur, A. G.; Abbas, A.; Fathifazl, G.; Foo, S.; and Isgor, O. B., "Shear Strength of Reinforced Recycled Concrete Beams with Stirrups," *Magazine of Concrete Research*, V. 62, No. 10, 2010, pp. 685-699. doi: 10.1680/macr.2010.62.10.685

14. Choi, W. C., and Yun, H. D., "Compressive Behavior of Reinforced Concrete Columns with Recycled Aggregate under Uniaxial Loading," *Engineering Structures*, V. 41, 2012, pp. 285-293. doi: 10.1016/j.engstruct.2012.03.037

15. Corinaldesi, V., and Moriconi, G., "Behavior of Beam-Column Joints Made of Sustainable Concrete under Cyclic Loading," *Journal of Materials in Civil Engineering*, ASCE, V. 18, No. 5, 2006, pp. 650-658. doi: 10.1061/(ASCE)0899-1561(2006)18:5(650)

16. Corinaldesi, V.; Letelier, V.; and Moriconi, G., "Behaviour of Beam-Column Joints Made of Recycled-Aggregate Concrete under Cyclic Loading," *Construction and Building Materials*, V. 25, No. 4, 2011, pp. 1877-1882. doi: 10.1016/j.conbuildmat.2010.11.072

17. Xiao, J. Z.; Sun, Y. D.; and Falkner, H., "Seismic Performance of Frame Structures with Recycled Aggregate Concrete," *Engineering Structures*, V. 28, No. 1, 2006, pp. 1-8. doi: 10.1016/j.engstruct.2005.06.019

18. Xiao, J. Z.; Wang, C. Q.; Li, J.; and Tawana, M. M., "Shake-Table Model Tests on Recycled Aggregate Concrete Frame Structure," *ACI Structural Journal*, V. 109, No. 6, Nov.-Dec. 2012, pp. 777-786.

19. Priestley, M. J. N.; Sritharan, S. S.; Conley, J. R.; and Pampanin, S., "Preliminary Results and Conclusions from the PRESSS Five-Storey Precast Concrete Test Building," *PCI Journal*, V. 44, No. 6, 1999, pp. 42-67. doi: 10.15554/pcij.11011999.42.67

20. Khoo, J.; Li, B.; and Yip, W., "Tests on Precast Concrete Frames with Connections Constructed away from Column Faces," *ACI Structural Journal*, V. 103, No. 1, Jan.-Feb. 2006, pp. 18-27.

21. Xue, W., and Yang, X., "Tests on Half-Scale, Two-Story, Two-Bay, Moment-Resisting Hybrid Concrete Frames," *ACI Structural Journal*, V. 106, No. 5, Sept.-Oct. 2009, pp. 627-635.

22. Alcocer, S. M.; Carranza, R.; Perez-Navarrete, D.; and Martinez, R., "Seismic Tests of Beam-to-Column Connections in a Precast Concrete

Frame," *PCI Journal*, V. 47, No. 3, 2002, pp. 70-89. doi: 10.15554/pcij.05012002.70.89

23. Psycharis, I. N., and Mouzakis, H. P., "Assessment of the Seismic Design of Precast Frames with Pinned Connections from Shaking Table Tests," *Bulletin of Earthquake Engineering*, V. 10, No. 6, 2012, pp. 1795-1817. doi: 10.1007/s10518-012-9372-9

24. Jaillon, L., and Poon, C. S., "Design Issues of Using Prefabrication in Hong Kong Building Construction," *Construction Management and Economics*, V. 28, No. 10, 2010, pp. 1025-1042. doi: 10.1080/01446193.2010.498481

25. Tam, V. W.; Tam, C. M.; Zeng, S. X.; and Ng, W. C., "Towards Adoption of Prefabrication in Construction," *Building and Environment*, V. 42, No. 10, 2007, pp. 3642-3654. doi: 10.1016/j.buildenv.2006.10.003

26. Soutsos, M. N.; Tang, K. K.; and Millard, S. G., "Use of Recycled Demolition Aggregate in Precast Products, Phase II: Concrete Paving Blocks," *Construction and Building Materials*, V. 25, No. 7, 2011, pp. 3131-3143. doi: 10.1016/j.conbuildmat.2010.12.024

27. Soutsos, M. N.; Tang, K. K.; and Millard, S. G., "The Use of Recycled Demolition Aggregate in Precast Concrete Products—Phase III: Concrete Pavement Flags," *Construction and Building Materials*, V. 36, 2012, pp. 674-680. doi: 10.1016/j.conbuildmat.2012.06.045

28. Xiao, J. Z.; Huang, X.; and Shen, L. M., "Seismic Behavior of Semi-Precast Column with Recycled Aggregate Concrete," *Construction and Building Materials*, V. 35, 2012, pp. 988-1001. doi: 10.1016/j.conbuildmat.2012.04.062

29. Xiao, J. Z.; Pham, T. L.; Wang, P. J.; and Gao, G., "Behaviors of Semi-Precast Beams Made of Recycled Aggregate Concrete," *Structural Design of Tall and Special Buildings*, V. 23, No. 9, 2014, pp. 692-712. doi: 10.1002/tal.1071

30. ACI Committee 318, "Building Code Requirements for Structural Concrete (ACI 318-05) and Commentary," American Concrete Institute, Farmington Hills, MI, 2005, 430 pp.

31. Sonin, A. A., "A Generalization of the Π-theorem and Dimensional Analysis," *Proceedings of the National Academy of Sciences of the United States of America*, V. 101, No. 23, 2004, pp. 8525-8526. doi: 10.1073/pnas.0402931101

32. Seismology Committee, "Recommended Lateral Force Requirements and Commentary (Blue Book)," Structural Engineers Association of California (SEAOC), Sacramento, CA, 1999, pp. 327-421.

33. Structural Engineers Association of California (SEAOC) Performance-Based Seismic Engineering Ad Hoc Subcommittee, "Revised Interim Guidelines: Performance-Based Seismic Engineering for the SEAOC Blue Book," Sacramento, CA, 2003, pp. 128-132.

34. Belén, G. F.; Fernando, M. A.; Diego, C. L.; and Sindy, S. P., "Stress-Strain Relationship in Axial Compression for Concrete Using Recycled Saturated Coarse Aggregate," *Construction and Building Materials*, V. 25, No. 5, 2011, pp. 2335-2342. doi: 10.1016/j.conbuildmat.2010.11.031

35. Park, R., and Paulay, T., *Reinforced Concrete Structures*, John Wiley & Sons, Inc., New York, 1975, 769 pp.

36. Rahman, M. A., and Sritharan, S., "Performance-Based Seismic Evaluation of Two Five-Story Precast Concrete Hybrid Frame Buildings," *Journal of Structural Engineering*, ASCE, V. 133, No. 11, 2007, pp. 1489-1500. doi: 10.1061/(ASCE)0733-9445(2007)133:11(1489)

37. Stanton, J.; Stone, W. C.; and Cheok, G. S., "A Hybrid Reinforced Precast Frame for Seismic Regions," *PCI Journal*, V. 42, No. 2, 1997, pp. 20-23. doi: 10.15554/pcij.03011997.20.23

38. Belleri, A., and Riva, P., "Seismic Performance and Retrofit of Precast Concrete Grouted Sleeve Connections," *PCI Journal*, V. 57, No. 1, 2012, pp. 97-109. doi: 10.15554/pcij.01012012.97.109

39. Park, R., "Evaluation of Ductility of Structures and Structural Assemblages from Laboratory Testing," *Bulletin of the New Zealand National Society for Earthquake Engineering*, V. 22, No. 3, 1989, pp. 155-166.

40. Park, Y. J., and Ang, A. H. S., "Mechanistic Seismic Damage Model for Reinforced Concrete," *Journal of Structural Engineering*, ASCE, V. 111, No. 4, 1985, pp. 722-739. doi: 10.1061/(ASCE)0733-9445(1985)111:4(722)

41. Park, Y. J.; Ang, A. H. S.; and Wen, Y. K., "Seismic Damage Analysis of Reinforced Concrete Buildings," *Journal of Structural Engineering*, ASCE, V. 111, No. 4, 1985, pp. 740-757. doi: 10.1061/(ASCE)0733-9445(1985)111:4(740)

42. Xiao, J. Z.; Lu, D.; and Ying, J. W., "Durability of Recycled Aggregate Concrete: An Overview," *Journal of Advanced Concrete Technology*, V. 11, No. 12, 2013, pp. 347-359. doi: 10.3151/jact.11.347